PROBING THE LIMITS - NEW OPPORTUNITIES IN THERMOELASTIC STRESS ANALYSIS

Nik Rajic , David Rowlands , Steve Galea
Defence Science and Technology Organisation
nik.rajic@dsto.defence.gov.au;
david.rowlands@dsto.defence.gov.au;steve.galea@dsto.defence.gov.au

Keywords: *thermoelasticity, microbolometer, infrared, fatigue, SHM*

Abstract

This article outlines the development, validation and application of a novel thermoelastic stress analysis (TSA) system based on a low-cost and low-grade microbolometer detector. The system is the first of its kind and represents a radical departure from commercial systems, which employ highly sensitive cryogenically cooled photonic detectors. Despite using a markedly inferior detector the system achieves performance levels that are comparable to its commercial counterparts, but at a fraction of the capital cost and in a smaller, more rugged and portable package. It is hoped this development might assist in revitalising interest in TSA and help expand its use across a range of important engineering applications, including support to airframe structural integrity management. A full-scale fatigue test of a flight-critical aircraft structural component is employed as a case study to demonstrate important aspects of this capability and to point to possible future directions in its development and application.

1 Introduction

Thermoelastic Stress Analysis (TSA) is one of only a few methods capable of furnishing a full-field measurement of mechanical stress. Yet, despite the commercial availability of TSA systems for over thirty years, and the advent of rapid staring-array systems almost twenty years ago [1], the contemporary use of TSA is not as widespread as might have been reasonably anticipated several decades ago. Indeed, awareness of the method seems to be declining as its role is gradually displaced by optical techniques such as digital image correlation (DIC) and electronic speckle pattern interferometry (ESPI). These methods certainly have an important role to play, but TSA is far from obsolete. Indeed, it offers superior stress sensitivity as well as other practical advantages that should see an expansion of its role in experimental stress-analysis. The reasons for its modest uptake remain a matter for conjecture and debate, however two contributing factors are reasonably clear: (i) the relatively high capital cost of commercial TSA systems, and (ii) a perception that the technology is impractical and difficult to use. The affordability of TSA hardware has improved significantly over the past decade, however this hasn't had the anticipated effect on uptake of the technology, arguably because it has occurred at a relatively low ebb in general awareness of the method, so to some extent has gone unnoticed. Recent advancements in microbolometer technology provide an opportunity for a more radical reduction in capital cost as well as providing a more rugged and compact imaging platform, the combination of which has the potential to transform TSA into an affordable mainstream technique with a much wider scope of potential application than previously considered possible with available commercial systems. The present ar-

ticle outlines briefly the development, validation and application of a system that realises these goals. The system, named MiTE (Microbolometer ThermoElasticity), was developed by the Australian Defence Science and Technology Organisation (DSTO) and is based on a low-grade microbolometer detector. This detector is the antithesis of the highly-sensitive photonic detectors traditionally used for stress analysis applications. Yet, as this article will show, the MiTE system achieves a level of performance that is comparable to commercial systems and seemingly out of proportion to its relatively poor detector specifications. The system was first reported in [2], however that article was devoid of any technical details. The present paper fills in the gaps, providing a more detailed albeit still brief account of the development and validation of the system as well as its application to several aircraft structural integrity problems. One of these, involving an F/A-18 full-scale fatigue test article, provides a particularly effective illustration of the practical advantages of the MiTE system over its commercial photonic counterparts, and of the potential that then arises for TSA to contribute to structural integrity assessments across the full life-cycle of an engineering asset, from basic design and validation [3] to through-life maintenance. It also suggests a prospect for the emergence in future of a structural health monitoring (SHM) capability based on a network of in situ miniaturised microbolometer cameras.

2 Thermoelasticity

Detailed reviews of the thermoelastic effect and TSA can be found in [3] and [4] for example, so only a brief summary of the fundamentals is necessary here. The thermoelastic effect describes a small reversible change in the temperature of an object when it undergoes an elastic deformation. Gough [5] was first to report an observation of the effect in 1805. A theoretical description was reported by Lord Kelvin in 1853 [6]. The relationship is given by [7],

$$\delta T = \frac{-3T_o\alpha_T K\delta\varepsilon}{\rho C_v} \tag{1}$$

where δT is the change in temperature produced by a change in bulk strain $\delta\varepsilon$, T_o is the absolute temperature, α_T is the coefficient of thermal expansion, K is the bulk modulus, ρ is the mass density, and C_v is the specific heat at constant volume. In terms of bulk stress ($\delta\sigma$) the relationship is;

$$\delta T = \frac{-\alpha_T T_o\delta\sigma}{\rho C_p} \tag{2}$$

where C_p is the specific heat at constant pressure. A few fundamental properties of the effect are immediately apparent. Firstly, only a dilatational deformation produces a thermoelastic response. Secondly, a positive change in stress (increasingly tensile) produces a negative change (drop) in temperature, and vice versa. Thirdly, the relations describe a reversible phenomenon, meaning that a material deformed and then released is expected to recover its initial thermal state exactly. For that to occur the deformation must take place adiabatically. Since strain gradients produce temperature gradients, and loading rates are invariably finite, adiabatic conditions are never strictly attained in practice. However, a satisfactory working approximation can be achieved if the stress varies dynamically at a rate high enough to limit the time available for heat diffusion. Static loading represents a limiting case where the thermoelastic response is extinguished by diffusion. The temperature changes produced by the thermoelastic effect are relatively small - typically under 500mK. A radiometric measurement of temperature variations on this scale is not trivial, and largely explains why the effect remained unexploited for stress analysis until the latter part of the 1970's. The sensitivity, or noise equivalent temperature detectivity (NETD) of a modern photonic detector is typically no better than 15 mK. In aluminium, this equates to a change in stress of approximately 5 MPa, or about 70 $\mu\varepsilon$. A standard electrical-resistance strain-gauge typically does much better.

3 Microbolometers

The NETD of a microbolometer is at least 4 times higher than for an average photonic detector, so the measurement challenge is clearly more difficult. This fundamental difference, along with a much longer integration time, might explain the preference shown by commercial system vendors for photonic detectors. However, neither of these factors pose a strict impediment to the development of a useful TSA capability. Indeed, the authors contend that for a large number of applications the difference in stress-measurement performance is not significant, and moreover the practical advantages of a low capital cost, rugged construction and compact size would likely outweigh shortfalls stemming from an inferior detector specification. The TSA system described in the present article was developed using a FLIR A20M (see Fig. 1) which is a low-grade commercial microbolometer camera that by photonic detector standards has exceptionally poor performance specifications. The A20M contains a Vanadium Oxide (VOx) focal-plane array with $160(\mathrm{H}) \times 120(\mathrm{V})$ detector cells, and has a rated NEDT of 120 mK, which is almost one order of magnitude higher than that of a cooled Indium Antimonide (InSb) detector, and over twice that of present generation microbolometer detectors. Output from the detector is in 16 bit digital form and is supplied at a fixed frame rate of 50 Hz.

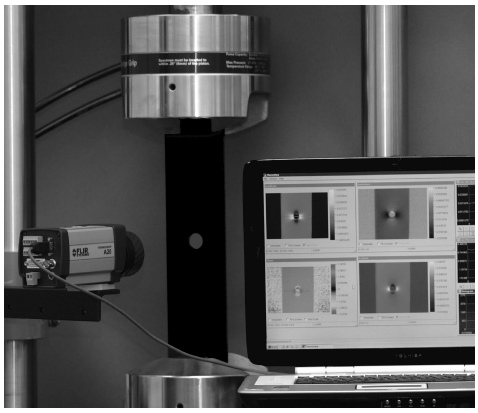

Fig. 1 MiTE system in action analysing a hole-in-plate coupon.

4 Sensitivity Enhancement

An NETD of 120 mK equates to a stress measurement noise floor in aluminium of approximately 44 MPa, a value that suggests a poor basis for developing a precise stress measurement capability. It turns out that is not the case. Providing the load signal is known, and the noise in the radiometric signal is chiefly temporal and random, the threshold stress measurement sensitivity can be improved significantly with rudimentary signal processing. Consider an applied load that varies harmonically in time, viz.,

$$L(t) = L_o e^{j\omega t} \tag{3}$$

where L_o is the load amplitude and ω is the circular frequency. Equation 2 is linear so the thermoelastic response occurs at the same frequency[1]. If the loading is sufficiently rapid to negate the effects of diffusion, and the structure is not at resonance, the thermoelastic response can be written as [8],

$$T(x,y,t) = A(x,y).(L(t) - \overline{L}) + B(x,y) \tag{4}$$

where $\overline{L}$ is the temporal average of the load, B accounts for any background infrared emission uncorrelated with the load, and the constant of proportionality A is a function of the material properties, which are normally known, and the stress amplitude, which is sought. A least squares estimate for the constant A is obtained by minimising the function,

$$\chi = \sum_{k=1}^{N} (T_k^{n,m} - A^{n,m} L_k - B^{n,m})^2 \tag{5}$$

where the subscript k is an index to time, the superscripts n,m identify the detector cell, N is the number of temporal samples and L is the oscillatory component of the load (i.e. stripped of its offset). This produces the set of equations,

[1] A response also occurs at the second harmonic but is much weaker and can be ignored for the present exercise.

$$\begin{pmatrix} \sum L_k^2 & \sum L_k \\ \sum L_k & \sum 1 \end{pmatrix} \begin{pmatrix} A^{n,m} \\ B^{n,m} \end{pmatrix} = \begin{pmatrix} \sum L_k T_k^{n,m} \\ \sum T_k^{n,m} \end{pmatrix}. \tag{6}$$

Since L_k varies about a zero mean, it follows that,

$$A^{n,m} = \frac{\sum L_k T_k^{n,m}}{\sum L_k^2}. \tag{7}$$

Equation 7 describes a cross-correlation between the radiometric and load signals. The process works remarkably well in removing uncorrelated noise. Indeed, where the noise in the measurement $T^{n,m}$ is random Gaussian, the standard deviation in $A^{n,m}$ declines as a function of $\sqrt{N}$. That property has an important and obvious corollary. It suggests that the NETD, which is mostly a measure of the temporal noise floor of a detector, and is a critically important parameter in conventional infrared imaging, has little bearing on TSA performance. Typically, the limiting factor on performance is fixed-pattern spatial noise (see for example [9]). Such noise stems from variations in the offset and gain characteristics across the detector cells in a focal plane array [10] and occurs in both photonic and microbolometer imagers. Variations in the detector gain are the most important since these are indistinguishable from variations in the thermoelastic response in the scene (i.e. are correlated with the load signal), and appear as a bias in the estimate $A^{n,m}$, which establishes a true noise floor, i.e. one that is immune to cross-correlation. The non-uniformity of an array is readily corrected using a two-point calibration against a uniform scene, however the gain and offset values are not stable so the correction needs to be applied periodically to maintain optimal noise performance.

5 System Implementation

Equation 7 assumes a synchronous acquisition of the infrared data stream and the load reference signal. This is relatively straightforward to achieved in practice if a framegrabber is employed. However, the use of dedicated hardware was ruled out for the present implementation because of the adverse impact on system affordability, size and ruggedness, as well as the increased risk of obsolescence. Those considerations led to a decision to base development of the system on an off-the-shelf notebook computer. Only two specific requirements were imposed: that it contain an integrated IEEE1394 interface to allow for a direct acquisition of the digital infrared signal from the A20M, and a PCMCIA slot to accommodate an analog to digital converter (ADC) for the acquisition of the load reference signal. Incidentally, the ADC is the only peripheral device in the system dedicated to the TSA process.

The pursuit of a low-cost and compact hardware configuration raises some technical challenges. As anticipated, an analysis of the load and infrared signals acquired using this arrangement revealed the presence of a significant time delay. This finding, along with other considerations meant that a real-time computation of the correlation sums was impractical. A pseudo-real-time approach was used instead. The sums were calculated off-line in a piecewise continuous process using stored blocks of data, and then recursively averaged over the full length of the test. Corrections for various time delays, described shortly, were implemented as part of that process. The approach takes marginally longer than a real-time computation, but the difference is largely negligible, since at the loading frequencies typically employed in TSA ($\approx 1-20\,\mathrm{Hz}$) data acquisition accounts for the bulk of the total analysis time.

The process was tested using an experimental apparatus comprising a small Peltier cell driven harmonically by a function generator. A relatively low drive frequency of 1.5 Hz was required to accommodate the slow thermal response time of the Peltier cell. The value $A^{n,m}$ was computed for an arbitrarily chosen detector cell (n,m) as a function of the number of temporal samples, or image frames. Figure 2 plots the decline in signal noise. The trend is approximately log-linear, and the improvement in sensitivity after 10,000 samples is nearly two orders of magnitude, which accords with expectation. The result was achieved with just over 3 minutes of processing and the im-

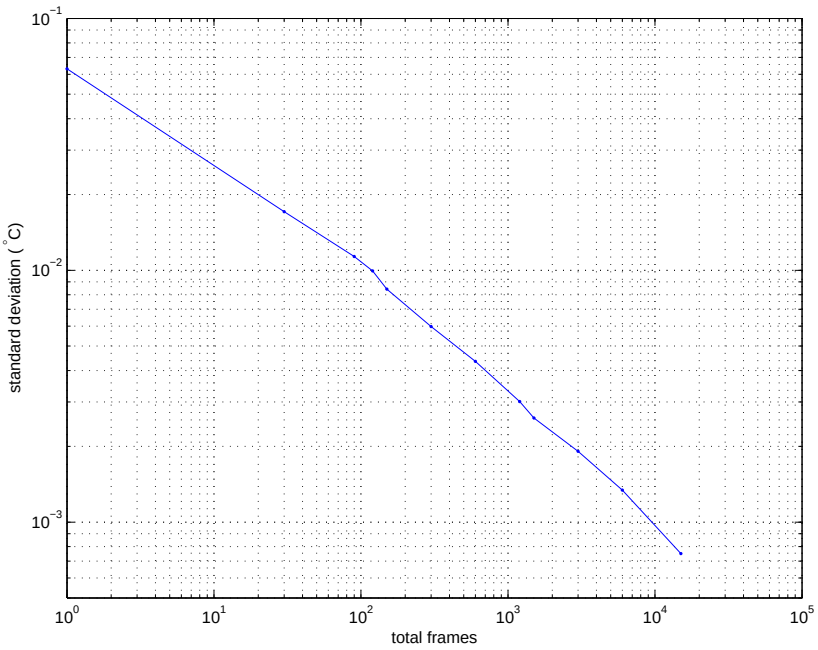

Fig. 2 Improvement in sensitivity with processing time.

proved noise floor translates to a stress measurement sensitivity in aluminium of below 1 MPa.

Recall from Equation 2 that an adiabatic thermoelastic response is precisely antiphase relative to the load signal. In practice, some deviation in that phase relationship will invariably occur due to the effects of heat transfer, mainly conduction within the sample. However, in the present system the load and infrared signals are skewed by an unknown system delay, which adds an extraneous phase variation. In fact, the system introduces three delays. These can be expressed in terms of an adjustment to the phase of the load signal, which is re-written as follows,

$$L^{n,m}(t) = L_o\, e^{j\omega t}\, e^{-\phi_{tc}}\, e^{-\phi_{td}}\, e^{-\phi_{sd}^{n,m}} \qquad (8)$$

where ϕ_{tc} denotes a phase delay due to the detector integration process, ϕ_{td} refers to a transport delay between sampling of the load and infrared signals, and ϕ_{sd} describes a scan delay between detector cells in the array. Each delay has a significant influence on the correlation process.

A detailed account of the measures required to characterise these delays and to compensate for them in the computation of the thermoelastic response is beyond the scope of the present article, however the reader interested in those details can refer to [11] for the relevant information.

6 Validation

A systematic validation of the capability was achieved by comparing observations furnished by the system with independent predictions provided by numerical and analytical methods. Again, a full account of the validation exercise is beyond the scope of the present article but is available elsewhere [11]. Here, we outline the key findings of one such exercise.

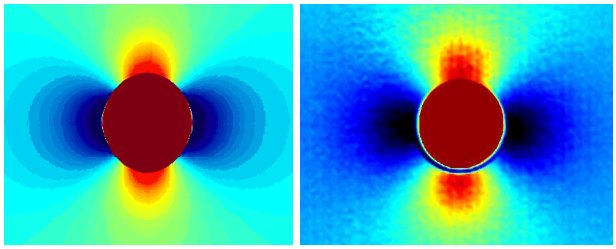

Fig. 3 Comparison of a prediction by FEA (left) with an observation furnished by MiTE (right). The case pertains to a plate with a circular hole exposed to uniaxial loading.

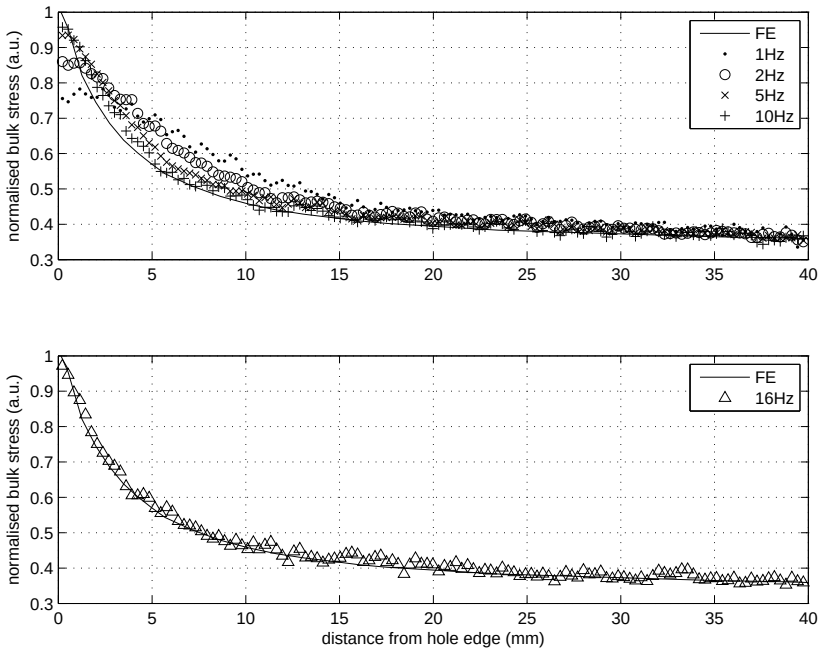

Fig. 4 Comparison of MiTE measurements against FEA predictions for a plate containing a circular hole.

Figure 3 compares a thermoelastic response measurement obtained from MiTE with a corresponding prediction from Finite Element Analysis (FEA). The results were derived from an investigation of an aluminium plate containing a circular hole and exposed to uniaxial loading in a mechanical test machine. The agreement is seen to be excellent, and is further confirmed in Figure 4 which compares the profile of the measured thermoelastic response to the bulk stress distribution from FEA along a line extending laterally from the hole edge. Measured traces are shown for several different loading frequencies. As the frequency increases the measured profile is seen to converge to the FEA result, and at 16 Hz the two are largely coincident suggesting that pseudo-adiabatic conditions have been achieved.

7 Airframe Lifing - An Illustration of System Embedment

Verification of airframe life in a military air fleet is typically established by means of a full-scale fatigue test (FSFT). That process is presently underway for the centre-barrel of the F/A-18A/B Hornet, as part of a mid-life structural upgrade for the Royal Australian Air Force (RAAF) fleet, which is aimed at ensuring the nominal safe life of the airframe (6000 hours) can be achieved [12]. The centre-barrel comprises

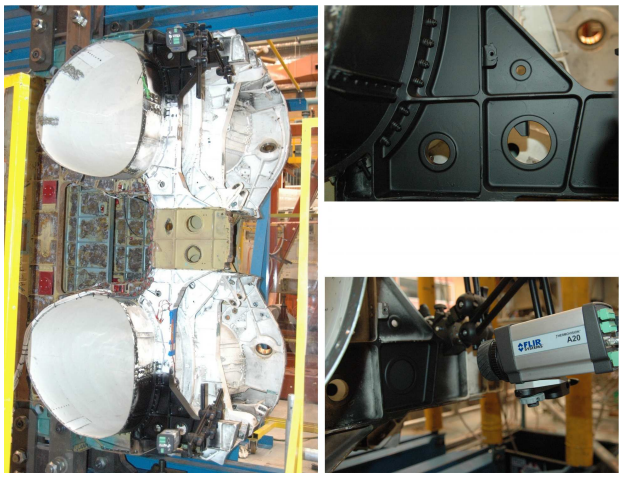

Fig. 5 TSA of the aft bulkhead in the Centre-Barrel of a Royal Australian Air Force F/A-18. Top right photograph shows a close-up of the hydraulic hole under inspection (arrowed). Bottom right photograph shows a close-up of the A20M fixed to the bulkhead.

three wing-attachment bulkheads machined from 7050-T7451 aluminium alloy plate. Figure 5 points out one of the structurally critical features in the centre-barrel, which is a hydraulic hole near the wheel well in the aft bulkhead. As part of the fatigue-life assessment process, an investigation by TSA was required to verify the fidelity of finite element modelling of this region.

The structure is subject to wing-root bending loads, which are applied at the wing-attachment points by means of a load frame connected to a pair of hydraulic actuators. Two aspects of the investigation are particularly worth noting. Firstly, the rig is incapable of applying constant amplitude loads above a frequency of about 1 Hz. Secondly, the displacement of the structure under load is large, especially near the upper wing-attachment points where the load is applied. Both pose a challenge for TSA. A relatively low loading rate exposes the analysis to bias due to heat conduction. Motion is potentially even more disruptive. An implied assumption in TSA is that displacements under load are negligibly small i.e. that the scene is effectively static. That assumption does not hold in the present case as displacements around the region of interest are in the range of tens of millimetres over a load cycle. A fixed observation from a standard tripod-mounted system would clearly prove unworkable. Motion compensation could be applied as an integral part of the cross-correlation process, and indeed that, arguably, would be the only feasible approach with a commercial system, but a more effective solution was available in the present case, by virtue of the compact size, low cost and ruggedness of the MiTE system. It was simply attached to the test article and permitted to move in unison with the scene (see close-up in Figure 5). Of course, it is possible to mount a cooled photonic imager in the same way, but the increased mass and size would necessitate a more cumbersome support arrangement, and the practitioner would need to be particularly risk tolerant and perhaps exceptionally well-funded given that structural failure of the component (which is not unlikely in the context of a FSFT) might lead to loss of the equipment.

Although the actual FSFT of the centre barrel is performed using a variable-amplitude flight-load sequence, for convenience the present analysis was conducted using a constant amplitude sinusoidal load at a frequency of 0.6 Hz. The peak load was limited to approximately 10% of the maximum value in the actual flight-load sequence.

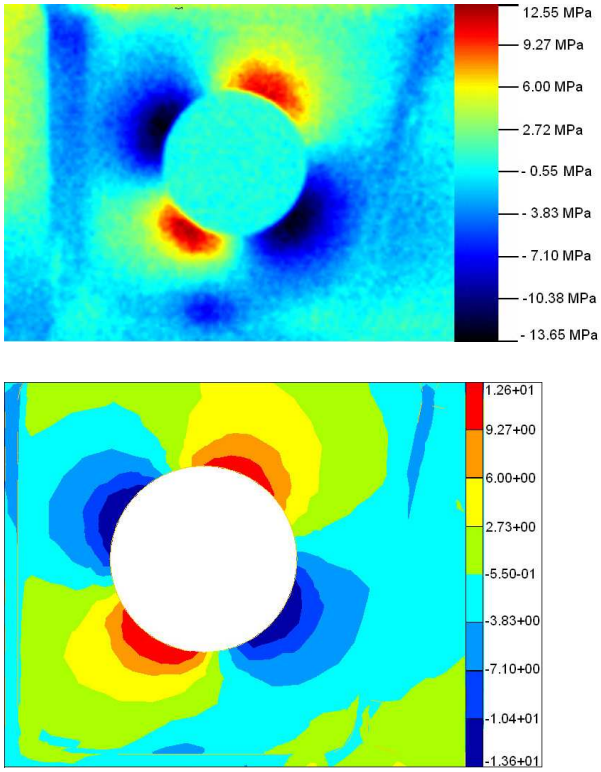

Fig. 6 Bulk stress distribution around the hydraulic hole arrowed in Figure 5, as assessed using MiTE (top) and predicted by FEA (bottom).

Figure 6 compares the stress distribution furnished by MiTE with the FEA prediction. The agreement is excellent, with peak tensile and compressive stress values matching remarkably well. It is to be noted that although the quadrature signal indicated the presence of heat conduction, the effect on the measurement was evidently small; probably mitigated by the relatively large size of the hole (≈ 57 mm) which has a scaling effect on the stress (and temperature) gradient.

8 Variable Amplitude Loading

While pure sinusoidal loading offers an experimentally convenient basis for TSA, and indeed is preferred for most laboratory investigations, it is not a necessity. Recall that an adiabatic thermoelastic response is linearly related to the load so the cross-correlation methodology described previously is valid for any load sequence that can be expressed as a sum of harmonic terms of the form of Equation 3. MiTe is no different to any other TSA system in this regard, but it is worthwhile providing some proof of its performance under these conditions. We again use an aircraft structural integrity application as the demonstration vehicle. The case considered involves a wing-skin coupon subject to a complex flight-load spectrum.

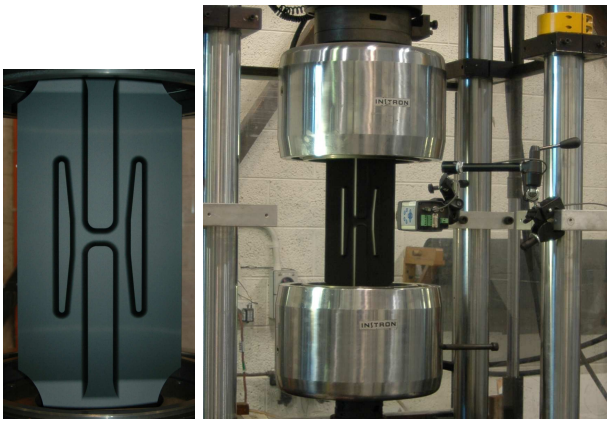

Fig. 7 An F-111 lower wing-skin FASS 281.28 coupon (left) with an arrow pointing to a fatigue-critical feature examined using MiTE (right).

The coupon, shown in Figure 7, accurately replicates the structural detail in a fatigue-critical section of the lower wing skin of the F-111C aircraft in a location known as FASS[2] 281.28. The key feature here is a depression in the main integral stiffener, the purpose of which is to facilitate fuel flow between adjacent bays of the wing-box fuel tank. It unfortunately also creates a large stress concentration which leads eventually to premature fatigue cracking [13].

The variable amplitude loading applied to the coupon was derived from an F-111C flight-load spectrum (or sequence). This sequence was stripped of all compressive loads for the present exercise since the coupon lacks the restraints to buckling found in the actual wing structure. Figure 8 shows part of the modified sequence as measured at the load-cell during an actual test, as well as the corresponding amplitude spectrum. The load-points in the sequence were applied to the coupon at a rate of two per second. For comparison purposes, an additional TSA was done under pure sinusoidal loading at an equivalent frequency (1 Hz) and rms equivalent amplitude. Figure 9 shows the measured stress distributions, which are virtually identical. In each case, the test duration was approximately 6 minutes.

An analysis confined to the primary frequency in a variable amplitude load sequence ignores information that is potentially valuable. At the simplest level, response components close to the primary frequency could be used to improve the signal to noise ratio of a stress measurement. More significantly, a broad-band measurement of the thermoelastic response offers information that might help to retrieve an adiabatic response [11].

9 Future Directions - In Situ Structural Health Monitoring

The absence of cryogenic cooling in microbolometer detectors enables a degree of hardware miniaturisation that is simply not possible with photonic detectors. Indeed, miniature microbolometer cameras not much larger than a match-box have been commercially available for a little over a decade. Given the mass-market opportunities in consumer-electronic devices it is reasonable to expect that miniaturisation of infrared imagers will continue as a trend in the foreeseable future. The implications for TSA could be significant and the F/A-18 centre barrel application described previously illustrates how. In that case an in-situ multi-site inspection was

[2]Forward Auxillary Spar Station.

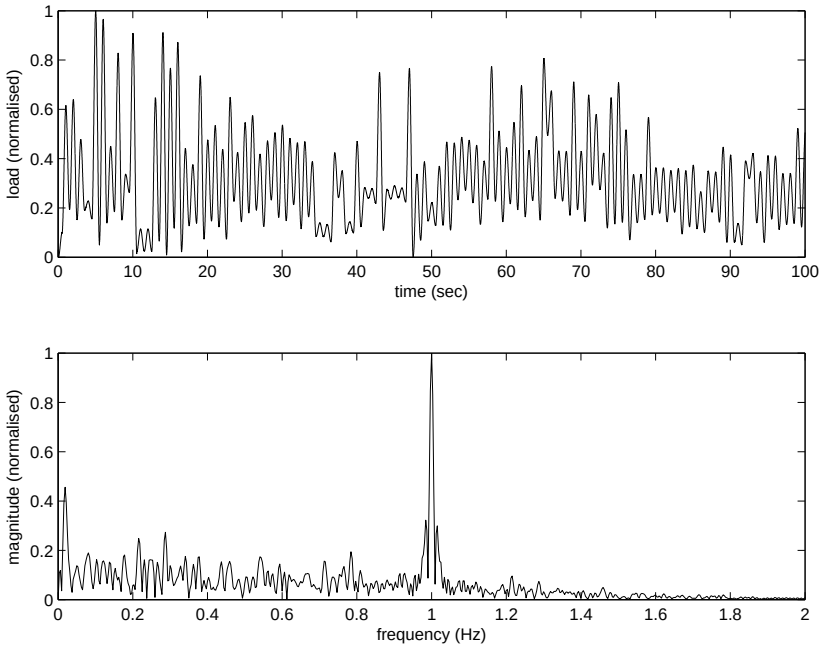

Fig. 8 Sample of a modified flight-load spectrum applied to the FASS 281.28 coupon (top), and its magnitude spectrum (bottom).

possible only because of the low-cost, compact size and ruggedness of the MiTE system. From there it takes only a small conceptual leap to imagine a ubiquitous in situ network of miniature cameras that could conceivably furnish a constant stream of information about the stress state and structural integrity of any engineering asset. The concept is clearly useful in FSFT programs, as demonstrated in the F/A-18 example, and particularly if applied in the way suggested in [3], however it has broader potential for in-service applications, where it could provide a uniquely powerful basis for in situ structural health monitoring (SHM). In furnishing a measurement of stress, TSA provides information that can be applied for structural management across the full life-cycle of an asset, from furnishing load information for life prediction, to in situ detection and monitoring of cracks, and finally to aid prognostic assessments. Few SHM methods offer this breadth of potential capability.

10 Conclusion

This article has described the development, validation and application of a novel thermoelastic

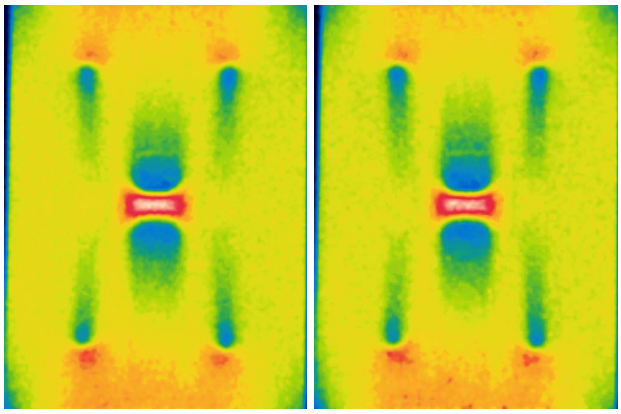

Fig. 9 Results from MiTE obtained under a variable amplitude flight-load spectrum (left) and pure sinusoidal loading (right).

stress analysis system based on a low-cost microbolometer detector. Several experimental case studies were employed to validate the system and to illustrate some of its unique aspects. Its performance across those case studies was shown to be excellent, which underscores that an effective TSA capability can be achieved without the use of a high-cost photonic detector. In many practical situations a microbolometer detector might actually be preferred because of its relatively

low-cost, compact size, rugged construction and lower energy requirements. It is hoped that the development of this facility will make TSA more broadly accessible and foster its more widespread use within the engineering community.

Acknowledgment

The contribution of Mr Matt Pelosi to the mechanical testing is gratefully acknowledged.

Copyright Statement

References

[1] T. G. Ryall and A. K. Wong, "Infrared Staring Arrays and Digital Signal Processing," in *Proc. SEM 50th Annual Spring Conference on Experimental Mechanics, Michigan, USA*, pp. 730–739, June 1993.

[2] N. Rajic, S. Weinberg, and D. Rowlands, "Low-cost Thermoelastic Stress Analysis," *Materials Australia*, vol. 40, 2007.

[3] A. Wong, "Making the Invisible Visible: Joining the Dots from Lord Kelvin to Fighter Jet Fatigue," in *Proc. 28th Congress of the International Council of the Aeronautical Sciences* (P. I. Grant, ed.), 2012.

[4] J. M. Dulieu-Barton and P. Stanley, "Development and Applications of Thermoelastic Stress Analysis," *The Journal of Strain Analysis for Engineering Design*, vol. 33, no. 2, pp. 93–104, 1998.

[5] J. Gough *Manchester Phil. Mem.*, vol. 2, pp. 288–295, 1805.

[6] W. Thomson *Trans. R. Soc. Edinburgh*, vol. 20, pp. 261–283, 1853.

[7] N. Harwood and W. M. Cummings, *Thermoelastic Stress Analysis*. Adam Hilger, Bristol, 1991.

[8] T. G. Ryall and A. K. Wong, "Design of a Focal-Plane Array Thermographic System for Stress Analysis," *Experimental Mechanics*, vol. 35, pp. 144–147, 1995.

[9] A. K. Wong and T. G. Ryall, "Performance of the FAST System for Stress Analysis," *Experimental Mechanics*, vol. 35, pp. 148–152, 1995.

[10] L. Shkedy, O. Amir, Z. Calahorra, J. Oiknine-Schlesinger, and I. Szafranek, "Temperature dependence of spatial noise in InSb focal plane arrays," in *Proc. SPIE 4028*, pp. 481–488, 2000.

[11] N. Rajic and D. Rowlands, "Thermoelastic Stress Analysis with a Compact Low Cost Microbolometer System," *submitted Experimental Mechanics*, 2012.

[12] G. Swanton and L. Robertson, "Developments with the F/A-18 FINAL Centre Barrel Test Program," in *Proceedings of AIAC14 - The Fourteenth Australian International Aerospace Congress, Melbourne, Australia*, 2011.

[13] R. Boykett and K. F. Walker, "F-111C Lower Wing Skin Bonded Composite Repair Substantiation Testing," Tech. Rep. DSTO-TR-0480, 1996.